Self-Assembled Fluorescent and Antibacterial GHK-Cu Nanoparticles for Wound Healing Applications

Leming Sun, Aipeng Li, Yanzi Hu, Yang Li, Li Shang, and Lianbing Zhang*

GHK-Cu is demonstrated with the abilities to improve wound healing, accelerate anti-inflammatory activity, and repair DNA damage. However, the instability of the GHK-Cu in biological fluids is always a big challenge for its long-term and efficient function at the target site. Therefore, the self-assembled GHK-Cu nanoparticles (GHK-Cu NPs) are investigated in this work to solve the instability issue. The crystalline nanostructure within the GHK-Cu nanoparticles offers them visible and near-infrared fluorescent properties. With the excellent self-assembly performance, the antibacterial properties of GHK-Cu NPs are demonstrated using *E. coli* and *S. aureus*. The L929 dermal fibroblast cells are utilized to prove the good biocompatibility and enhanced wound healing applications of GHK-Cu NPs. This study could pave the way for the design and elaboration of a new class of fluorescent peptides with various biological functions in biomedical applications.

The tripeptide glycyl-L-histidyl-L-lysine (GHK) has been demonstrated for applications in wound healing of skin, bone, intestine, blood vessels, and nervous tissue since its discovery in 1973.[1] It normally presents in human saliva, plasma, and urine. The unique regenerative capacity of GHK was founded due to their concentration decrease from 200 ng mL^{-1} at age 20 to 80 ng mL^{-1} at age 60 in human plasma.[1] The subsequent studies stated that the wound healing and anti-aging properties of GHK were due to their strong affinity for copper ions (Cu^{2+}) to form the GHK-Cu complex.[2] Many studies have proved the enhanced properties of GHK-Cu for wound healing, anti-inflammation, and DNA damage repair after cancer therapy, comparing with GHK.[3–5] Moreover, GHK-Cu has been noticed for their potential applications in metastatic colon cancer,

chronic obstructive pulmonary disease, and anti-aging cosmetic products.[6–8]

Although GHK-Cu has so many well-investigated biological activities and interesting functions, its instability in biological fluids is always a big challenge for its long-term and efficient use as a therapeutic agent.[9,10] In order to overcome this problem, peptide self-assembly can be a potential method that may introduce many attractive properties including structural programmability, low immunogenicity, low cost, good biodegradability, and biocompatibility.[11–15] Peptide self-assembly is a thermodynamic and kinetic-driven process involving intermolecular noncovalent interactions, including hydrophobic, hydrogen bonding, electrostatic, π–π stacking, and van der Waals interactions.[11,16] As a useful fabrication approach, peptide self-assembly can be utilized to create many different architectures such as nanoparticles, nanotubes, nanowires, nanofibers, and hydrogels.[17–22] These self-assembled structures have the potential to overcome the instability problems due to their aggregation mechanisms and spatial arrangements. Moreover, peptide nanomaterials with different shapes and functions have various potential applications in drug delivery, tissue engineering, biosensor, nanodevices, and energy.[17,23–28]

Peptide self-assembly strategy not only has the ability to form different nanostructures with well-demonstrated biological properties but also supply new features such as fluorescence and conductivity.[29–34] These new discoveries have attracted more and more attention recently in material science and biomedical fields.[35–39] For instance, inspired from the red shift in the yellow fluorescent protein (YFP) and improved fluorescence intensity in the green fluorescent protein (GFP) mutant BFPms1, tryptophan-phenylalanine dipeptide was self-assembled into nanoparticles with blue fluorescent signal due to the π–π stacking and zinc coordination.[37,40] These biocompatible and photostable dipeptide nanoparticles have been demonstrated for targeted cancer cell imaging and real-time monitoring of drug release.[37] Near-infrared (NIR) fluorescent peptide nanoparticles were also obtained through the self-assembly of cyclic octa-peptides.[36] People have discovered that not only the aromatic peptides have the potential to self-assembly into fluorescent peptide nanomaterials but also the nonaromatic peptides could form intrinsic visible fluorescence.[41] The GHK-Cu peptides have similar key components including amino acids and metal ions as the GFP mutant BFPms1 that contribute to the generation of fluorescent properties.[40]

Dr. L. Sun, Dr. A. Li, Y. Li, Prof. L. Zhang
School of Life Sciences
Key Laboratory of Space Bioscience & Biotechnology
Northwestern Polytechnical University
Xi'an 710072, China
E-mail: lbzhang@nwpu.edu.cn

Y. Hu
College of Chemistry and Chemical Engineering
Xi'an Shiyou University
Xi'an 710065, China

Prof. L. Shang
School of Materials Science and Engineering
Center for Nano Energy Materials
Northwestern Polytechnical University
Xi'an 710072, China

The ORCID identification number(s) for the author(s) of this article can be found under https://doi.org/10.1002/ppsc.201800420.

1800420 (1 of 6)

Therefore, the peptide self-assembly strategy can be a promising method to overcome the instability of GHK-Cu monomers and enhance their original functions with new features such as fluorescence. This new function could offer them a controlled release of GHK-Cu at wound sites with intradermal drug retention probed by fluorescence.

To verify this proposal, in this study, the peptide self-assembly strategy was applied to fabricate GHK-Cu nanoparticles (GHK-Cu NPs) with different reaction conditions. The nanomorphology, size distribution, and crystalline structure of GHK-Cu NPs were investigated for the understanding of their self-assembly process and correlations with fluorescent properties. The antibacterial, biocompatible, and wound healing activities were also studied to explore the advantages of the self-assembled GHK-Cu NPs including stability and wound healing potentials.

GFPs and their mutants such as YFPs and blue fluorescent proteins (BFPs) have regarded as one of the most widely utilized proteins due to their intrinsic visible fluorescent properties. From previous studies, the most important discoveries are the physical extent of π–π stacking contained within the chromophore, which is the most important factor to determine the general spectral types such as cyan, green, yellow, and red. However, there are also many other factors such as hydrophobic interactions, position of charged amino acid residues, and hydrogen bonding network within the protein matrix that can generate either blue or red spectral shifts in the absorption and emission.[42] The GHK-Cu peptides have the similar amino acids Glycine (G) and Histidine (H) in the chromophore as in BFPs, and the Lysine (K) residues also could supply extra charged amino acids for the generation of fluorescence.[43] Moreover, in the BFPs, not only the zinc coordination but also the copper coordination have the ability to enhance the fluorescent intensity.[40] Therefore, inspired from the molecular mechanisms described above, the GHK-Cu monomers were self-assembled into nanoparticles with potential fluorescent properties through hydrogen bonding and copper coordination (**Figure 1**).

After the self-assembly process, the morphology, size distribution, elements, and crystalline structure of the self-assembled GHK-Cu NPs were characterized and the results were shown in **Figure 2** and Figure S1 in the Supporting Information. The HRTEM and atomic force microscopy (AFM) images demonstrated the morphology of the GHK-Cu NPs with a diameter of around 15 nm (Figure 2A,C). It is noteworthy that

layered structures existed in GHK-Cu NPs based on HRTEM (Figure 2B), which revealed the appearance of supramolecular stacked structures inside the peptide nanoparticles. Moreover, the X-ray diffraction (XRD) spectrum results (Figure 2D) with distinct sharp peaks and high intensities also stated the well-ordered nanocrystal structure of the GHK-Cu NPs. The size distribution of GHK-Cu NPs analyzed with dynamic lighting scattering (DLS) (Figure 2E) also confirmed the uniform 15 nm sized GHK-Cu NPs were synthesized successfully in this study. The energy-dispersive X-ray (EDX) results (Figure S1, Supporting Information) stated that before and after the self-assembly, both of the GHK-Cu monomers and NPs have the same elements. All these results demonstrated that the uniform GHK-Cu NPs were successfully fabricated through a noncovalent self-assembly process.

People have demonstrated that aromatic peptides could be assembled into quantum wells that exhibit visible and NIR fluorescence.[35] The quantum-confinement phenomena were believed to occur because of the presence of the crystalline structure at the sub-nanometer scale. In this study, the similar crystalline structure was also discovered by the previous HRTEM and XRD results. The fluorescent emission spectra of the GHK-Cu monomers and GHK-Cu NPs are shown in **Figure 3**A,B. With the 375 nm excitation wavelength, only the GHK-Cu NPs showed remarkable blue fluorescent with emission wavelength around 435 nm and no obvious fluorescence could be observed by monomeric GHK-Cu under the same excitation wavelength (Figure 3A). Moreover, the results in Figure 3B demonstrated the synthesis of NIR fluorescent GHK-Cu NPs with emission wavelength around 830 nm. The fluorescent intensities of GHK-Cu NPs with 375 nm excitation wavelength are lower than the fluorescent intensities with 435 nm excitation wavelength. Combined with the fluorescent results in Figure 3A, it could be proposed that the GHK-Cu NPs could be excited by 375 nm and give a 435 nm emission at stage I. Since the 435 nm excitation wavelength also has the capacity to trigger the GHK-Cu NPs with an 830 nm emission, the 435 nm emission wavelength from stage I could be utilized as the excitation wavelength and induced the similar 830 nm emission. It has also been proposed that the intrinsic fluorescence may be independent of the presence of aromatic side-chain residues within the polypeptide structure.[44] Recently, the unique intrinsic visible emission from nonaromatic amino acids and polypeptides have been observed. The conformation rigidification and 3D electronic communication channels
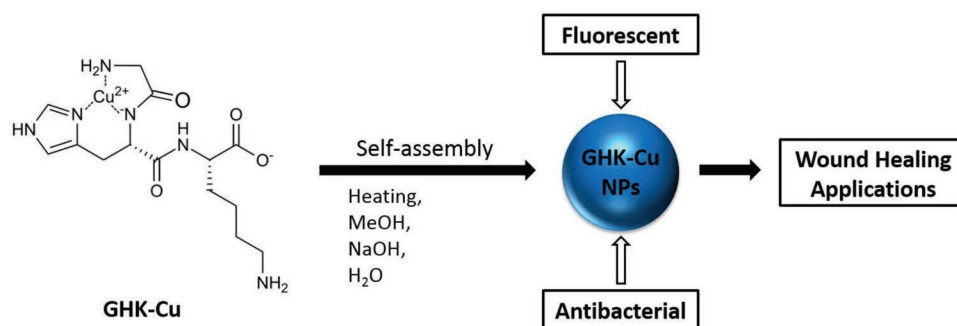

Figure 1. The self-assembly scheme toward fluorescent and antibacterial GHK-Cu nanoparticles (GHK-Cu NPs) for wound healing applications.

**ADVANCED
SCIENCE NEWS**
www.advancedsciencenews.com

Particle
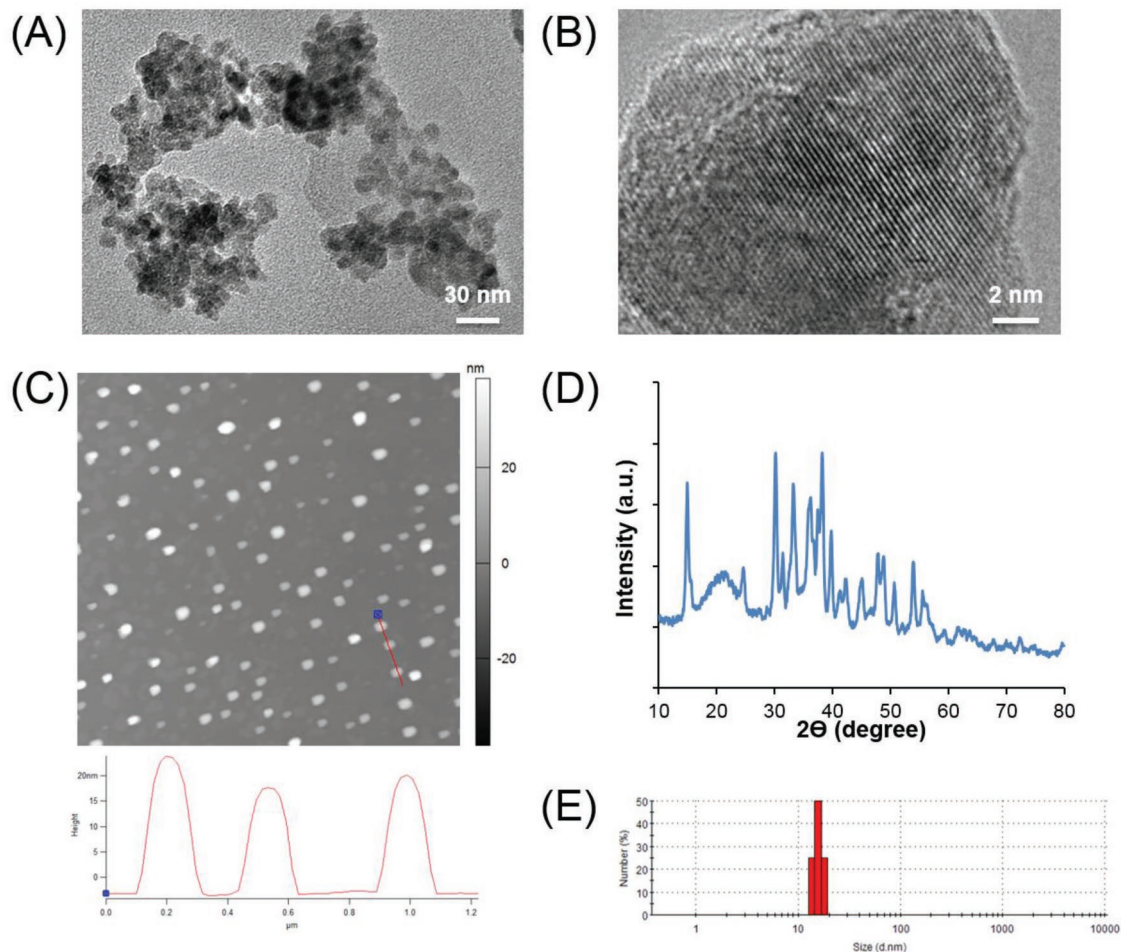& Particle Systems Characterization
www.particle-journal.com

Figure 2. A,B) Representative HRTEM images of GHK-Cu NPs, AFM image and correlated height line of (C) GHK-Cu NPs, (D) XRD and (E) DLS results of GHK-Cu NPs.

are believed to be essential for the extended delocalization, and thus emission of the nonaromatic amino acids and polypeptides.[41] Thus, the hydrogen bonding and metal ions coordination could contribute to the fluorescence redshift. However, the limited intrinsic optical properties of peptides have substantially restrained their potential applications.[45] The fluorescence properties of GHK-Cu NPs also have been identified in Figure S2 in the Supporting Information and Figure 3C. The aggregated GHK-Cu NPs in dry format showed clear blue color using the confocal microscope. The L929 cells were also utilized to verify the blue fluorescence properties of GHK-Cu NPs in Figure 3C. The negative control and GHK-Cu monomers showed no fluorescence performance. In this study, the fluorescent results have demonstrated that the self-assembled GHK-Cu NPs can shift the peptide's intrinsic fluorescent signal from UV to visible and even NIR ranges. Therefore, the peptide self-assembly strategy could offer GHK-Cu more opportunities in many applications such as in optical and biomedical fields.

The antibacterial activities and biocompatibility are critical for the wound healing applications.[46] As shown in Figure 3D and Figure S3 in the Supporting Information, compared to GHK-Cu monomers, the self-assembled GHK-Cu NPs showed obvious inhibition zones for both *Escherichia coli* (*E. coli*) and

Staphylococcus aureus (*S. aureus*). The deionized water was utilized as the negative control. These results could be due to the self-assembly strategy, which formed uniform and tight nanostructures with aggregated GHK-Cu inside of them. The nanoparticle form of GHK-Cu is more condensed and maybe more efficient at the target sites to inhibit the bacterial growth and survival. Moreover, this result also demonstrated that the GHK-Cu NPs could be more stable than the GHK-Cu monomers and so they can have a better antibacterial performance at the same concentration. The previous studies have stated that the GHK-Cu monomers are unstable in the biological fluids due to enzymatic degradation.[47] Therefore, the self-assembly process improves the stability and enhances the biological functions of the GHK-Cu. The cytotoxicity of GHK-Cu NPs was investigated using an L929 cell with 0, 10, 50, 100 µg mL−1, and 1, 10 mg mL−1 samples after 24 h of incubation. Up to 1 mg mL−1, no obvious cytotoxic effect was observed for dermal fibroblast cells (Figure 3E; Figure S4, Supporting Information). These demonstrated good antibacterial activity and biocompatibility of the GHK-Cu NPs will have great benefits for biomedical applications, especially wound healing.

To investigate the potential wound healing applications of GHK-Cu NPs, the wound scratch assay was utilized in this study.
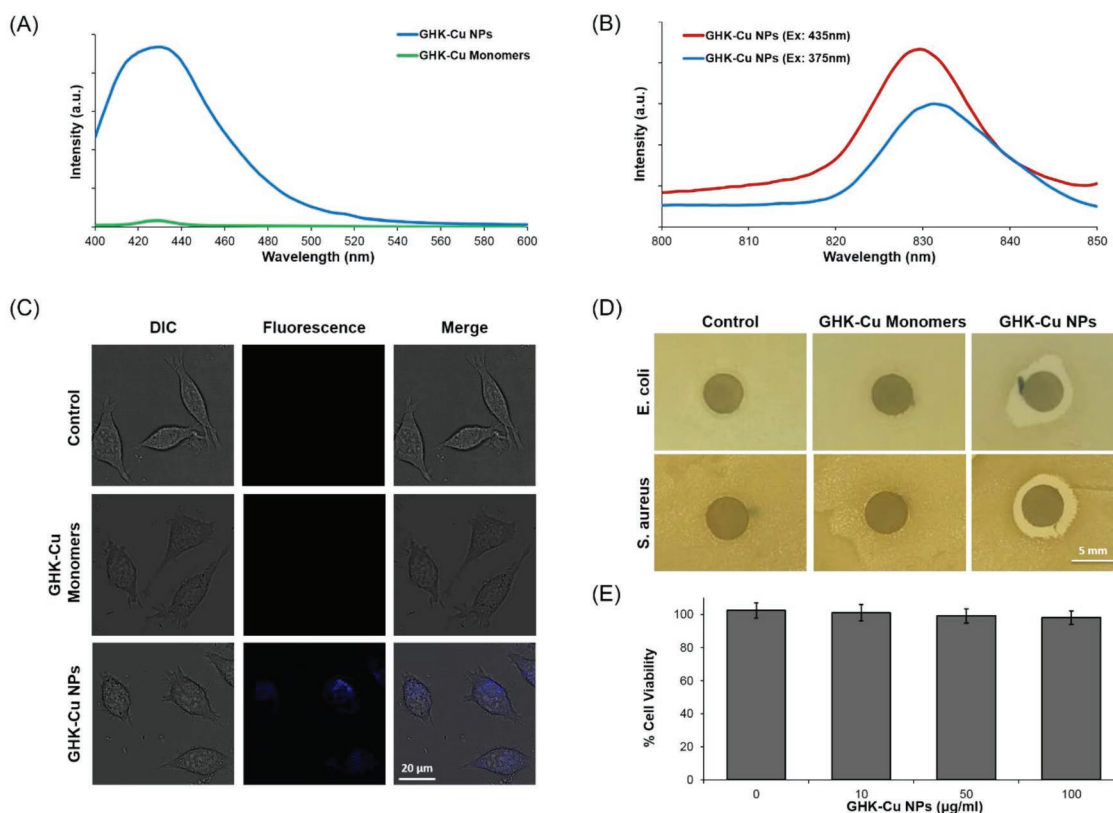
Figure 3. A) The visible fluorescent properties of GHK-Cu NPs and GHK-Cu monomers, and (B) NIR fluorescent properties of GHK-Cu NPs. C) The fluorescence properties of the control, GHK-Cu monomers, and GHK-Cu NPs in L929 cells using a confocal microscope . D) The antibacterial properties of the control, GHK-Cu monomers and GHK-Cu NPs . E) The biocompatible properties of GHK-Cu NPs.

Cell migration is a rate-limiting event in the wound-healing process.[48] Therefore, we examined how the GHK-Cu NPs affected dermal fibroblast migration during the wound contraction and healing process. The scratch assay method was used with L929 dermal fibroblasts to evaluate wound closure in vitro. In L929 dermal fibroblast cells, the GHK-Cu NPs enhanced wound closure the most (around 45%) compared to the GHK-Cu monomers (around 17%) and control (around 5%) at the 12 h time point (**Figure 4**). Moreover, by 24 h, nearly complete wound closure of L929 fibroblasts treated with GHK-Cu NPs was observed. However, the wound closure for GHK-Cu monomers (around 37%) and control (around 16%) was far away from the complete stage. Differences between the percent of wound closure and speed of wound closure observed with GHK-Cu NPs and GHK-Cu monomers treatment was likely due to the form of GHK-Cu peptides. The instability of the GHK-Cu monomers in biological fluid could be the main reason for the difference compared to GHK-Cu NPs. In other words, these results could be the evidence that the peptide self-assembly strategy overcomes the instability of GHK-Cu peptides in biological fluids for their long-term and efficient function at the target site.

In summary, the self-assembled fluorescent and antibacterial GHK-Cu nanoparticles not only overcome the instability of GHK-Cu peptides in biological fluids for their delivery and performance but also can give them new features, such as fluorescence, with great potential in biomedical fields. The morphological and structural studies revealed the uniform

15 nm GHK-Cu NPs with crystalline structures, which are also correlated with their visible and NIR fluorescent properties. The antibacterial and cytotoxicity investigations demonstrated the antibacterial GHK-Cu NPs with good biocompatibility. The wound healing potentials of GHK-Cu NPs were verified by the wound scratch assays using L929 dermal fibroblasts. The antibacterial and wound healing studies not only demonstrate the better stability properties of GHK-Cu NPs compared to their monomers but also the enhanced wound healing potentials. The self-assembly approach demonstrated in this work may be used as a general method for the development of various functional polypeptidic nanomaterials with great promising applications in drug delivery, tissue engineering, and cosmetic applications.

Experimental Section

Materials: GHK-Cu monomers were purchased from GL Biochem (Shanghai) Ltd., China. Sodium hydroxide (NaOH) and methanol (MeOH) were purchased from Sinopharm Chemical Reagent Co., Ltd, China. All reagents used in this study were analytic reagent (AR)-grade and used as received. CCK-8 Cytotoxicity Kit was purchased from Life Technology (USA). Gram-positive bacterium *S. aureus* and Gram-negative bacterium *E. coli* were purchased from the Guangdong Institute of Microbiology. L929 cells were purchased from China Infrastructure of Cell Line Resources (Beijing, China).

Preparation of GHK-Cu NPs: GHK-Cu peptides were dissolving in a mixed solution with NaOH, H$_2$O, and MeOH. The volume ratio between pure MeOH and 1 M NaOH was 9:1. The reaction solutions were heated
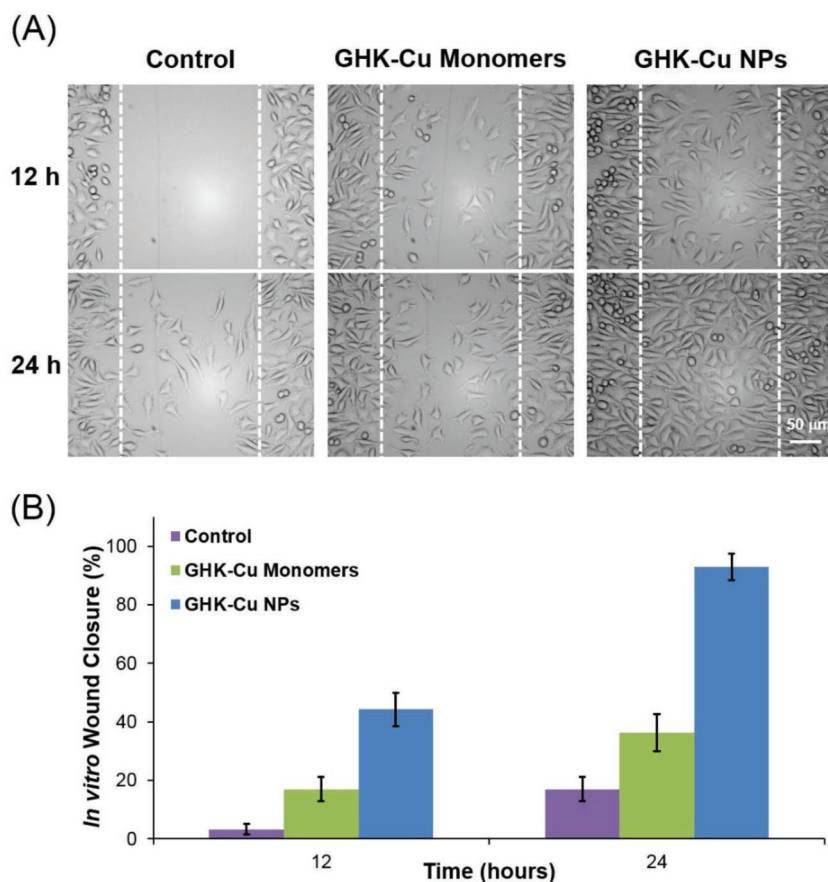
(A)

(B)

Figure 4. The wound scratch assay results of control, GHK-Cu monomers, and GHK-Cu NPs using L929 cells (A) and (B).

to 85 °C until all the MeOH was evaporated (when the volume reduced to around 1/10). Then the centrifugation process (8000 g, 10 min) was applied to purify the self-assembled GHK-Cu NPs. The GHK-Cu NPs were dispersed in deionized water for further analysis.

Material Characterization: Carbon-coated copper grids were utilized for the high-resolution transmission electron microscopy characterization. Ten microliters of GHK-Cu NPs (1 mg mL^{-1}) was dropped on the surface of the grids and dried at room temperature. The morphological structure of GHK-Cu NPs was characterized using FEI Talos F200X HRTEM at 80 kV. The nanomorphology of the GHK-Cu NPs was studied using a Bruker Dimension Icon AFM. A silicon tip on nitride level with the 4 N m^{-1} spring constant and 70 kHz resonant frequency was utilized in a tapping mode. Ten microliters of GHK-Cu NPs (1 mg mL^{-1}) was added on a cover glass and dried at room temperature for 24 h before the characterization. The crystalline structures of GHK-Cu NPs were characterized by XRD using a SHIMADZU XRD700 in a reflection mode. The analysis was performed with scan angles from 10° to 80° at a scan speed of 2 min^{-1}. MDI Jade software was utilized to collect and analyze the results. FE-SEM (TESCAN) equipped with INCA was applied to obtain the EDX spectra of GHK-Cu NPs and monomers. The DLS was performed through a Zetasizer Nano ZS (Malvern Instruments). The size distribution of GHK-Cu NPs was obtained in a 1 mL glass cuvette and operated at 25 °C with a backscattering angle of 173°. The analysis was performed three cycles for accuracy.

Fluorescence Characterizations: The fluorescence spectrophotometer (Leng Guang Tech F97XP) was applied to obtain the fluorescence excitation and emission spectra. The slit widths of excitation and emission were set at 5 nm. Three measurements were operated and averaged for accuracy. The fluorescence of the GHK-Cu NPs was identified by the confocal laser scanning microscopy platform (Leica TCS SP8). The L929

cells were cultured in the glass-bottom dish. The 10 µg mL^{-1} GHK-Cu NPs and monomers were added to the cells and cultured 30 min before washing and changing with new cell culture medium. The PBS was utilized as the negative control. After 1 h total culture, the fluorescence images were captured with x63 oil immersion objective. The optical (DIC), fluorescence, and merged images were utilized for the analysis.

Antibacterial Evaluation: Antibacterial activity of the GHK-Cu monomers and self-assembled GHK-Cu NPs was performed by the standard disc diffusion method.[49–51] The overnight grown bacterial suspensions of *S. aureus* and *E. coli* were swabbed on separate nutrient agar plates using L-rod. The 5 mm diameter filter paper discs were separately impregnated with 10 µL of 1 mg mL^{-1} solution of GHK-Cu monomer, GHK-Cu NPs, and 10 µL deionized water as negative control. The discs with samples were evaporated and impregnated on the bacterial plates. The bacterial cultures were incubated at 37 °C for 24 h and triplicates were maintained.

Biocompatibility Characterization: The cytotoxicity of GHK-Cu monomers, self-assembled GHK-Cu NPs was assessed in L929 cells using CCK-8 assay. Cells were first seeded into 96-well plates at a density of 10 000 cells per well. The L929 cells were then incubated for 2 h at 37 °C to permit cell adhesion. After that, the cells were then maintained in 100 µL of culture medium with three separate samples of GHK-Cu monomers, self-assembled GHK-Cu NPs, and deionized water as negative control. Following 12 and 24 h incubations, 10 µL of CCK-8 solution was added to each well and plates were incubated for an additional 4 h. Absorbance was measured at 450 nm by a microplate reader (Thermo Scientific Multiskan GO) and cell viabilities were compared to those of the control groups. All measurements were performed in triplicate.

Wound Healing Study: Once the L929 dermal fibroblast cells were grown confluent, the cell monolayer was scratched in a straight line using a sterile pipet tip to mimic an incision wound. Cells were then washed with PBS to remove debris. The cells were treated with GHK-Cu monomers, self-assembled GHK-Cu NPs, and deionized water as a negative control and incubated at 37 °C. The final concentrations of GHK-Cu monomers and nanoparticles were 100 µg mL^{-1}. Wound closure was monitored by collecting digitized images at various time intervals after the scratch was performed and until closure was either complete or no longer progressing. Digital images were captured under an inverted microscope (BFM800E, Bi Mu Inc., Shanghai, China), and the area of the scratch was analyzed using the Image-J software. Data presented represent the extent of wound closure (percentage by which the original scratch area has decreased for each given time point). Measurements were done in three replicate wells for each condition.

Supporting Information

Supporting Information is available from the Wiley Online Library or from the author.

Acknowledgements

ADVANCED
SCIENCE NEWS
www.advancedsciencenews.com

Particle
& Particle Systems Characterization
www.particle-journal.com

Conflict of Interest

The authors declare no conflict of interest.

Keywords

[1] L. Pickart, J. M. Vasquez-Soltero, A. Margolina, *Biomed. Res. Int.* **2015**, *2015*, 648108.
[2] T. Badenhorst, D. Svirskis, Z. Wu, *Pharm. Dev. Technol.* **2016**, *21*, 152.
[3] S. Sharma, A. Dua, A. Malik, *J. Polym. Res.* **2017**, *24*, 104.
[4] B. Reddy, T. Jow, B. M. Hantash, *Exp. Dermatol.* **2012**, *21*, 563.
[5] J. J. Hostynek, F. Dreher, H. I. Maibach, *Inflammation Res.* **2011**, *60*, 79.
[6] L. Pickart, *J. Biomater. Sci., Polym. Ed.* **2008**, *19*, 969.
[7] S. Meiners, O. Eickelberg, *Genome Med.* **2012**, *4*, 70.
[8] Y. Hong, T. Downey, K. W. Eu, P. K. Koh, P. Y. Cheah, *Clin. Exp. Metastasis* **2010**, *27*, 83.
[9] Y. Zheng, Q. Huo, P. Kele, F. M. Andreopoulos, S. M. Pham, R. M. Leblanc, *Org. Lett.* **2001**, *3*, 3277.
[10] V. Arul, D. Gopinath, K. Gomathi, R. Jayakumar, *J. Biomed. Mater. Res., Part B* **2005**, *73B*, 383.
[11] J. Wang, K. Liu, R. Xing, X. Yan, *Chem. Soc. Rev.* **2016**, *45*, 5589.
[12] C. Chen, K. Liu, J. Li, X. Yan, *Adv. Colloid Interface Sci.* **2015**, *225*, 177.
[13] A. L. Boyle, D. N. Woolfson, *Chem. Soc. Rev.* **2011**, *40*, 4295.
[14] S. Fleming, R. V. Ulijn, *Chem. Soc. Rev.* **2014**, *43*, 8150.
[15] K. H. Smith, E. Tejeda-Montes, M. Poch, A. Mata, *Chem. Soc. Rev.* **2011**, *40*, 4563.
[16] G. M. Whitesides, B. Grzybowski, *Science* **2002**, *295*, 2418.
[17] G. Colombo, P. Soto, E. Gazit, *Trends Biotechnol.* **2007**, *25*, 211.
[18] P. Zhu, X. Yan, Y. Su, Y. Yang, J. Li, *Chem. - Eur. J.* **2010**, *16*, 3176.
[19] J. Ryu, C. B. Park, *Adv. Mater.* **2008**, *20*, 3754.
[20] T. Fan, X. Yu, B. Shen, L. Sun, *J. Nanomater.* **2017**, *2017*, 16.
[21] L. Sun, Z. Fan, Y. Wang, Y. Huang, M. Schmidt, M. Zhang, *Soft Matter* **2015**, *11*, 3822.
[22] Y. Zhiqiang, X. Quan, D. Chenbo, L. Su Seong, G. Liqian, L. Yiwen, D. Mathew, Ortenzio, W. Jun, *Curr. Pharm. Des.* **2015**, *21*, 4342.
[23] C. A. E. Hauser, S. Zhang, *Nature* **2010**, *468*, 516.
[24] A. Kholkin, N. Amdursky, I. Bdikin, E. Gazit, G. Rosenman, *ACS Nano* **2010**, *4*, 610.
[25] Y. Wang, S. Yi, L. Sun, Y. Huang, S. C. Lenaghan, M. Zhang, *J. Biomed. Nanotechnol.* **2014**, *10*, 445.
[26] L. Sun, Z. Fan, T. Yue, J. Yin, J. Fu, M. Zhang, *Bio-Des. Manuf.* **2018**, *1*, 182.
[27] M. Abbas, R. Xing, N. Zhang, Q. Zou, X. Yan, *ACS Biomater. Sci. Eng.* **2018**, *4*, 2046.
[28] M. Yemini, M. Reches, E. Gazit, J. Rishpon, *Anal. Chem.* **2005**, *77*, 5155.
[29] Q. Chen, Y. Yang, X. Lin, W. Ma, G. Chen, W. Li, X. Wang, Z. Yu, *Chem. Commun.* **2018**, *54*, 5369.
[30] Y. Yang, X. Wang, G. Liao, X. Liu, Q. Chen, H. Li, L. Lu, P. Zhao, Z. Yu, *J. Colloid Interface Sci.* **2018**, *509*, 515.
[31] S. Xiang, P. Yang, H. Guo, S. Zhang, X. Zhang, F. Zhu, Y. Li, *Macromol. Rapid Commun.* **2017**, *38*, 1700446.
[32] C. Wang, D. Wang, T. Dai, P. Xu, P. Wu, Y. Zou, P. Yang, J. Hu, Y. Li, Y. Cheng, *Adv. Funct. Mater.* **2018**, *28*, 1802127.
[33] Y. Zou, L. Zhang, L. Yang, F. Zhu, M. Ding, F. Lin, Z. Wang, Y. Li, *J. Controlled Release* **2018**, *273*, 160.
[34] Y. Shi, X. Cao, D. Hu, H. Gao, *Angew. Chem.* **2018**, *130*, 525.
[35] K. Tao, Z. Fan, L. Sun, P. Makam, Z. Tian, M. Ruegsegger, S. Shaham-Niv, D. Hansford, R. Aizen, Z. Pan, S. Galster, J. Ma, F. Yuan, M. Si, S. Qu, M. Zhang, E. Gazit, J. Li, *Nat. Commun.* **2018**, *9*, 3217.
[36] Z. Fan, Y. Chang, C. Cui, L. Sun, D. H. Wang, Z. Pan, M. Zhang, *Nat. Commun.* **2018**, *9*, 2605.
[37] Z. Fan, L. Sun, Y. Huang, Y. Wang, M. Zhang, *Nat. Nanotechnol.* **2016**, *11*, 388.
[38] T. Yue, X. Jia, J. Petrosino, L. Sun, Z. Fan, J. Fine, R. Davis, S. Galster, J. Kuret, D. W. Scharre, M. Zhang, *Sci. Adv.* **2017**, *3*, e1700669.
[39] Z. Yu, Z. Cai, Q. Chen, M. Liu, L. Ye, J. Ren, W. Liao, S. Liu, *Biomater. Sci.* **2016**, *4*, 365.
[40] D. P. Barondeau, C. J. Kassmann, J. A. Tainer, E. D. Getzoff, *J. Am. Chem. Soc.* **2002**, *124*, 3522.
[41] C. Xiaohong, L. Weijian, M. Huili, P. Qian, Y. Wang Zhang, Z. Yongming, *Sci. China: Chem.* **2018**, *61*, 351.
[42] S. G. Olenych, N. S. Claxton, G. K. Ottenberg, M. W. Davidson, *Curr. Protoc. Cell Biol.* **2007**, *36*, 21.5.1.
[43] R. N. Day, M. W. Davidson, *Chem. Soc. Rev.* **2009**, *38*, 2887.
[44] F. T. S. Chan, G. S. Kaminski Schierle, J. R. Kumita, C. W. Bertoncini, C. M. Dobson, C. F. Kaminski, *Analyst* **2013**, *138*, 2156.
[45] M. R. Ghadiri, J. R. Granja, R. A. Milligan, D. E. McRee, N. Khazanovich, *Nature* **1993**, *366*, 324.
[46] Z. Lu, Z. Gao, Q. He, J. Wu, D. Liang, H. Yang, R. Chen, *Carbohydr. Polym.* **2017**, *156*, 460.
[47] M. Liakopoulou-Kyriakides, C. Pachatouridis, L. Ekateriuiadou, V. P. Papageorgiou, *Amino Acids* **1997**, *13*, 155.
[48] F. Cappiello, B. Casciaro, M. L. Mangoni, *JoVE* **2018**, e56825.
[49] G. Rajarathinam, S. Dronamraju, *Ind. Crops Prod.* **2013**, *51*, 107.
[50] J. Lin, J. Ding, Y. Dai, X. Wang, J. Wei, Y. Chen, *Mater. Sci. Eng., C* **2017**, *81*, 321.
[51] S. Li, S. Dong, W. Xu, S. Tu, L. Yan, C. Zhao, J. Ding, X. Chen, *Adv. Sci.* **2018**, *5*, 1700527.